Custom-designed, degradation-resistant messenger RNAs in yeast

Ana L. Franklin[1≠], Andrea Macfadden[2≠], Jeffrey S. Kieft[2,3], Jay R. Hesselberth[2,3], Erich G. Chapman[1*]

[1]Department of Chemistry and Biochemistry, University of Denver, Denver, CO 80208, USA

[2]Department of Biochemistry and Molecular Genetics, University of Colorado Denver School of Medicine, Aurora, Colorado, 80045, USA

[3]RNA Bioscience Initiative, University of Colorado Denver School of Medicine, Aurora, Colorado, 80045, USA

[≠]these authors contributed equally to this work

*To whom correspondence should be addressed:

Erich G. Chapman
Department of Chemistry and Biochemistry
University of Denver
2190 E. Iliff Ave.
F.W. Olin Hall, Room 202
Denver, CO 80208
Telephone: 303-361-3681
Fax: 303-871-2254
Email: erich.chapman@du.edu

Other author's contact info:

Ana L. Franklin
Telephone: 303-871-2287
Email: ana.franklin@du.edu

Andrea Macfadden
Telephone: 303-724-3256
Email: andrea.macfadden@ucdenver.edu

Jeffrey S. Kieft
Telephone: 303-724-3257
Email: jeffrey.kieft@ucdenver.edu

Jay R. Hesselberth
Telephone: 303-724-5384
Email: jay.hesselberth@gmail.com

Running head: Degradation resistant mRNAs

Keywords: Xrn1, xrRNAs, decay, degradation, resistance, IRES, yeast

ABSTRACT

Structured RNA elements that protect RNA transcripts from 5'→3' degradation are becoming useful research tools. Here we show that exonuclease-resistant RNA structures (xrRNAs) from Flaviviruses can be used to protect heterologous messenger RNAs (mRNAs) from 5'→3' degradation in budding yeast. Installation of xrRNAs ahead of a downstream internal ribosome entry site (IRES) leads to the accumulation of partially-degraded mRNAs that are substrates for cap-independent translation of a LacZ reporter, yielding a 30-fold increase in measured β-galactosidase activity. Additionally, by monitoring the translation of dual-luciferase reporters we show that xrRNA sequences do not interfere with the progression of an elongating ribosome. Combined these data indicate that xrRNA elements can be used in creative ways to stabilize RNAs with potentially useful applications.

INTRODUCTION

The levels of specific messenger RNAs (mRNAs) in cells correlate with levels of their respective proteins.[1,2] mRNA levels themselves are maintained by crosstalk between the interrelated processes of transcription and regulated mRNA decay.[3-6] Strategies to slow the degradation of specific mRNAs independent of increasing their transcription rates could therefore be useful for increasing corresponding protein expression levels. Potential tools for accomplishing this are viral RNA structures that resist 5'→3' degradation by the major eukaryotic exoribonuclease, Xrn1.[7,8] These exonuclease-resistant RNAs (xrRNAs) are found in the 3' untranslated region (3' UTR) of the positive-sense RNA genomes of Flaviviruses[9,10] and do not require a bound protein factor for function.[11] The flaviviral xrRNAs have been characterized structurally and biochemically,[7,8,11,12] and recent studies indicate that structurally diverse 5'→3' exonuclease-resistant RNA structures exist in other contexts within both the coding and non-coding regions of other positive-strand RNA viruses.[13-17] As an interesting aside, specific RNA-protein interactions have been shown to impede 5'→3' decay in both plants and animals as well.[18-20] Following our biochemical characterization of the flaviviral xrRNAs,[8,11] we gained interest in understanding how xrRNA structures could be used to control the degradation of specific mRNAs in other systems. Since we initiated these studies several other research groups have also recently reported similar ideas and strategies to protect RNAs from decay using flaviviral xrRNAs.[18,19] A key difference in this study is that we were interested in creating degradation-resistant *messenger* RNA species that retain their capability to be translated into functional proteins. Because the xrRNA-protected products produced by partial Xrn1 digestion bear a 5'-monophosphate rather than a type-0 5'-m^7GpppG cap,[11] they are not effective substrates for translation.

The design of degradation-resistant mRNAs that are translation-efficient therefore involved using a second viral RNA structure, the internal ribosomal entry site (IRES) domain from Cricket Paralysis virus (CrPV) which facilitates a streamlined, cap-independent mode of translation initiation using a mechanism involving structural mimicry of the tRNA-mRNA decoding interaction.[20,21] The CrPV IRES has been previously shown to function in a variety of organisms.[22-26] In this report we demonstrate that coupling of the tandem xrRNA structures found in the 3'UTR of the Dengue virus (DENV) to the CrPV IRES is capable of protecting heterologously expressed mRNAs in *Saccharomyces cerevisiae* (budding yeast) from 5'→3' exonucleolytic

decay and furthermore that the resulting protected mRNAs serve as effective templates for cap-independent translation originating from the CrPV IRES. The combined effects of the CrPV IRES and xrRNAs produce a significant enhancement in expression of a *lacZ* reporter. In related experiments, we inserted the DENV xrRNAs into the intergenic region of a dual luciferase reporter and discovered that xrRNA incorporation does not interfere with the progression of a translating ribosome. These results demonstrate an interesting difference between the helicase properties of the ribosome versus Xrn1. Cumulatively, our findings highlight the portability of viral RNA elements and the potential utility of combining functional RNAs from different viruses to engineer degradation-resistant mRNAs with potentially useful applications in regulating protein expression.

RESULTS AND DISCUSSION

Installation of xrRNA Structures in pre-mRNA Splicing Reporters

To test whether xrRNAs could be used to protect arbitrary mRNAs in yeast, we inserted the tandem xrRNA structures from a serotype 2 DENV virus into a series of previously characterized yeast pre-mRNA splicing reporters.[27] The plasmids that we used were most recently employed by Mayas, Staley and, co-workers to characterize the Dbr1/Xrn1-mediated decay pathway of splice-defective pre-mRNAs in yeast.[22]

As diagrammed in **Figures 1a,** the 2 micron-based reporters are bicistronic. In the parent pJPS-1481 reporter, transcription takes place from a GPD promoter producing mRNA species with a 91 nt 5' UTR, followed by exon 1 (ACT1a), the first intron, and 11 nucleotides of exon 2 (ACT1b) of the yeast ACT1 gene, terminated by a stop codon. The second region of the reporters encodes a CrPV IRES that is designed to drive cap-independent translation of a *LacZ* reporter. The reporter is trailed by the PGK1 3' UTR and includes several canonical polyadenylation sites. We hypothesized that the inclusion of xrRNA structures directly upstream of the CrPV IRES domain would result in the accumulation of the xrRNA-protected, partially-degraded RNA species in the pathway depicted in **Figure 1b**. In this model the xrRNA-protected degradation-resistant products that include the IRES domain and *lacZ* ORF are produced and should undergo ongoing cap-independent translation. To test the veracity of this model we compared the expression of three pre-mRNA splicing reporters: 1) the reporter pJPS-1481 that was inherited directly from a previous study by Mayas and

Staley 2) an xrRNA-modified reporter in which the tandem DENV xrRNA sequences (nt's 10274-10446 of Genbank accession M20558.1) were cloned into the BglII site in the parent reporter and 3) a version of the reporter in which structure-guided mutations to each xrRNA render them inoperable, pJPS-1481xrRNAs$_{mut}$ (nucleotides 10303-10305 AGU→UCA and 10377-10379 AGU→UCA in Genbank accession number M20558.1). Additional sequence information is included in **Figure S1.**

Accumulation of xrRNA-Protected Intermediates

We transformed plasmids encoding xrRNA-modified reporters into a yeast strain in which two out of the four genomic copies of initiator tRNA$_{met}$ genes (*imt3 imt4*) were deleted. These deletions reduce the expression of tRNA$_{met}$ which limits the formation of the eIF2-tRNA$_{met}$-GTP ternary complex used in cap-dependent translation, enabling the CrPV IRES to effectively compete for the translation machinery.[22] Using total RNA isolated from *imt3 imt4* yeast expressing our reporters, we carried out primer extension (PE) experiments to identify the build-up of 5'→3' decay intermediates. As shown in **Figure 2**, the inclusion of xrRNA structures results in the build-up of specific 5'→3' truncated, Xrn1-resistant RNA fragments (xrFrag$_1$, xrFrag$_2$).

Specifically, in lane 1 of the gel we observe primer-extension products corresponding to the unmodified, properly-spliced 1481 reporter at 689 nt, as well as a band corresponding to its pre-mRNA precursor at 387 nt. In lane 2 we observe similar spliced- and pre-mRNA products for the longer xrRNA-modified reporter at 862 and 560 nts respectively, as well as two robust bands corresponding to xrRNA-protected fragments xrFrag$_1$ and xrFrag$_2$ at 392 and 319 nts respectively. It is interesting that we observe fragments corresponding to Xrn1 resistance by each of the two DENV xrRNAs in yeast. This mirrors findings in other eukaryotic cell types that the installation of tandem xrRNA structures produces two distinct decay products corresponding to Xrn1 stalling at both the first and second of the xrRNA structures. This observation contrasts the quantitative stop at the first xrRNA structure, xrRNA1, that is observed in analogous experiments *in vitro*. Finally, in the last lane of the gel we see that a pair of 3 nt point mutations made within in the core of each xrRNA structure disrupt their structure and decay-resistance and fail to produce partially-degraded RNAs. Cumulatively, these results provide evidence that xrRNA structures can be installed in mRNAs in yeast, fold properly in the cell, don't interfere with splicing or nuclear export, and function outside of their natural context within the 3' UTR of the flaviviral genome.

Translation of xrRNA-Protected RNAs

To detect any increase in protein production related to the buildup of decay-resistant mRNAs, we used a β-galactosidase assay to monitor the enzymatic activity of lysates obtained from yeast cells expressing xrRNA-modified reporters (**Figure 3**). When yeast expressing JPS-1481 are lysed by repeated freeze-thaw cycles and analyzed for β-galactosidase activity using ortho-nitrophenyl-β-galactoside (ONPG), we observe OD_{420} values corresponding to 4.3 ± 1.6 Miller units of activity, representing a basal level of translation occurring from the IRES in transcripts subject to unimpeded decay. When lysates from yeast expressing the xrRNA modified reporter JPS-1481xrRNAs are assessed using the same assay, we measure 127.7 ± 22.0 miller units, an approximately 30-fold increase in enzymatic activity. Yeast expressing yJPS-1481xrRNAs$_{mut}$ show β-galactosidase activity similar to the parent construct at 5.0 ± 1.0 miller units. Combined with the aforementioned results that show the build-up of partially-degraded RNA fragments, these results suggest that the translation of xrRNA-protected, partially-degraded RNA species is responsible for increased protein expression in *imt*3 *imt*4 yeast.

To verify translation was indeed initiatiated from the CrPV IRES, we also tested two IRES-dead control vectors for β-galactosidase activity. The reporter pJPS-1482, as well as the analogous xrRNA-derivatized reporter pJPS-1482xrRNAs, encode mutations for two guanosines that are critical for the formation of a pseudoknot interaction in the IRES domain, specifically the interactions that mimics the tRNA-mRNA codon-anticodon interaction in cap-dependent translation (nt's G6214→C and G6215→C in the CrPV genome, Genbank accession KP974707.1). Yeast expressing pJPS-1482 or pJPS-1482xrRNAs produce with β-galactosidase activities of 4 ± 3.6 and 2.5 ± 1.2 Miller units respectively (**Figure 3**). Cumulatively, these results demonstrate that cap-independent translation of xrFrags leads to substantially more protein production from xrRNA-protected reporters versus unmodified or mutated controls.

xrRNA Structures Do Not Impede Translation When They Are Installed Within Open Reading Frames

Given our interest in incorporating xrRNAs into mRNAs, an interesting question became whether or not xrRNA structures could be unwound and translated through by an elongating ribosome. Though both are obligatory RNA helicases, the ribosome is a very different 5'→3' molecular machine than Xrn1. In order to test

whether xrRNA structures can be traversed by a translating ribosome, we employed a previously developed dual-luciferase reporter encoding an upstream firefly luciferase (FLUC), a modifiable linker region, and a downstream renilla luciferase (RLUC).[28] In these experiments cap-dependent translation of these reporters produces an RLUC-linker-FLUC fusion protein. The influence of specific RNA sequences and structures on translation is assessed by incorporating them into the linker region and monitoring changes in RLUC versus FLUC activity. [28] To assess the influence of xrRNA structures on progression of the ribosome, we generated the seven reporters shown in **Figure 4**. From top to bottom these constructs include: 1) the parent pYDL which produces an RLUC-linker-FLUC fusion protein, 2) a similar reporter with two stop codons after the FLUC sequence, pYDL-2xStop, 3) an xrRNA-modified version of the previous reporter, pYDL-2xStop-xrRNAs, 4) an xrRNA-modified version of the parent reporter pYDL-xrRNAs, 5) the previous construct with mutated xrRNAs, pYDL-xrRNAs$_{mut}$ 6) the pYDL plasmid with DENVxrRNA1 alone, pYDL-xrRNA1, and 7) and the pYDL plasmid with DENVxrRNA2 alone, pYDL-xrRNA2. The natural DENV xrRNA sequences contains three stop codons that were recoded by point mutations made in positions listed in the Materials and Methods. These do not compromise the decay resistance of the xrRNA structures themselves (**Figure S2**).

When yeast expressing these reporters are subjected to dual-luciferase assays we observe a base RLUC/FLUC value of 0.18 $\pm$ 0.02 for the parent pYDL reporter. Next, the addition of two stop codons in the linker region proceeding the RLUC open reading frame results in loss of RLUC expression, providing a negative control. Then, as predicted the incorporation of the tandem DENV xrRNAs behind the stop codon containing control similarly does not produce RLUC activity. For the xrRNA-modified reporter pYDL-xrRNAs, we observe an RLUC/FLUC ratio of 0.11 $\pm$ 0.01, a roughly 40% decrease from the control pYDL construct, indicating that the ribosome can indeed progress through the tandem DENV xrRNA structures. We then explored the translational capacity of several related constructs. The construct with mutated xrRNAs, pYDL-xrRNAs$_{mut}$ displayed RLUC/FLUC activity of 0.13 $\pm$ 0.01 that is not significantly different than pYDL-xrRNAs providing some indication the three-dimensional structures of the xrRNAs is not responsible for the attenuated RLUC/FLUC values observed when they are incorporated. Perhaps relatedly, installation of DENV xrRNA1 alone in the pYDL linker region produces RLUC/FLUC activity slightly higher than any of the constructs containing DENV xrRNA 2 sequence, including when it is installed alone in pYDL-xrRNA2. This leads us to

speculate that perhaps a rare codon within DENV xrRNA2 may attenuate translation, however this observation was not further pursued. Cumulatively, our results demonstrate that the ribosome is able to unwind and translate through xrRNA elements that resist being unwound and degraded by Xrn1. This portrays an interesting difference in how each molecular machine interacts with these unique RNA structures.

CONCLUSION AND SUMMARY

Experiments in the late 1970's described the dual role the mRNA cap structure plays in licensing translation and protecting against 5'→3' decay.[29,30] Here used two types of viral RNA elements together to provide these same capabilities in yeast. The observation that RNA structures from divergent positive-strand viruses operate together in an organism that is not a natural host for either of them is interesting and highlights the conservation of the RNA-decay and translational machinery across kingdoms.

Historically, a key question regarding overall gene expression has been the quantitative relationship between mRNA copy number and protein abundance in the cell.[1,2] Here we observe an increase in protein production attributable to the build-up of partially-degraded RNAs, however we did not directly quantify levels of either of these molecules. In the future, this type of question will gain in significance as efforts to advance new types of mRNA-based therapies and deliver them to cells gain traction. Regarding the use of xrRNA structures in these types of therapeutics- many current mRNA drug candidates incorporate modified nucleotides, 5mC or m6A and others, and it is unclear whether or not xrRNAs and other structured RNAs will operate properly when composed of modified nucleotides.

The observation that the ribosome, though not Xrn1, can progress through xrRNA structures encoded within an open reading frame demonstrates an interesting difference in the helicase properties of the two molecules. The ribosome's progression along an RNA transcript is coupled to the chemical energy released by hydrolysis of the high-energy phosphoanhydride bonds from two GTP molecules per translocation event. The mRNA being translated is threaded through an entry tunnel lined by multiple proteins and ribosomal RNA.[31-33] Recent single-molecule force spectroscopy experiments[31] indicate that the ribosome proceeds using an 'active' two-step mechanism, in which structurally, biochemical energy is applied to unwinding an incoming mRNA substrate.[34,35] The thermodynamic basis for Xrn1's helicase activity is less well understood, however it is not driven by NTP hydrolysis. Instead, the phosphodiester hydrolysis reaction that Xrn1 carries out is close to

enthalpically neutral (Welch and Chapman, *in preparation*). Lacking chemical energy from phosphodiester bond cleavage, Xrn1's helicase activity is instead proposed to result from a combination of Brownian motion and successive pi-stacking and electrostatic pull originating from the enzyme's active site.[36] These properties raise interesting questions regarding the biochemical basis for Xrn1's helicase activity and how it may account for the difference observed in how Xrn1 and the ribosome navigate through xrRNA structures installed within open reading frames.

Cumulatively, our findings indicate that xrRNA structures present a useful way to prevent the degradation of specific RNA substrates and when coupled to an IRES element provide a straight forward way to engineer translation-competent xrFrags capable of substantially increasing synthesis of functional protein.

ACKNOWLEDGEMENTS:

The authors thank Dr. Scott A. Barbee for critical reading of the manuscript and insightful comments and current and former members of the Chapman, Hesselberth and Kieft labs for thoughtful discussions and technical assistance. The expression vectors pJPS-1481 and pJPS-1482 were a gift from Dr. Jonathan Staley to JRH. H2545 yeast were a gift from Dr. Sunnie Thompson to JRH. pYDL plasmids were a gift from Dr. Jonathan Dinman to JRH. This work was supported by NIH grants R35GM118070 to JSK, R35GM119550 to JRH, and NIH K99GM115757 and R00GM115757 to EGC.

COMPETING INTERESTS:

AM, JSK, JRH and EGC are listed as inventors of PCT/US2016/066723 that describes this technology and its potential useful applications. This patent is owned by the Reagents of the University of Colorado.

MATERIALS AND METHODS:

Yeast Husbandry CRY1 (W303-1A, *MAT*a l*eu2-3,112 trp1-1 can1-100 ura3-1 ade2-1 his3-11,15*) and H2545 *(MATa trp1- 1 ura3–52, IMT1 IMT2 imt3::TRP1 imt4::TRP1 leu2::hisG GAL+)* yeast were maintained using standard yeast husbandry methods. Our recipe for 1 L of synthetic dropout (SD) minimal media includes 2 g synthetic drop-out mix (-His, -Leu, -Trp, -Ura) without nitrogenous base (US Biological cat. D9540), 1.7 g yeast nitrogenous base without amino acids, carbohydrate, or ammonium sulfate (US Biological cat. # Y2030), 5 g of ammonium sulfate, 10 ml of a 4 mg/ml tryptophan solution, 20 ml of an 8 mg/ml leucine solution, 5 ml of a 4 mg/ml histidine, and 865 ml water with 20 g agar added when preparing plates. This solution was autoclaved then supplemented with 100 ml of a sterile filtered 20% (w/v) glucose solution immediately prior to creating liquid cultures or pouring plates.

pJPS-1480 series plasmids: Yeast pre-mRNA splicing reporters were modified from reference [23]. Specifically, the plasmid pJPS-1481 and pJPS-1482 were modified for the studies included here. In order to insert xrRNAs into these constructs, the sequence of the tandem xrRNA structures found in the Jamaica/N.1409 strain, serotype 2 Dengue virus (GenBank accession number M20558.1, nt's 10272-10448) directly ahead of the

CrPV intergenic region (GenBank accession number KP974707.1, nt's 6025-6216), flanked on both ends by BglII restriction sites were ordered as a gBlock from Integrated DNA Technologies (IDT) and cloned in using standard restriction enzyme-based molecular cloning techniques.

pYDL series plasmids: The tandem DENV xrRNAs were analyzed for stop codons using an online translation tool (expasy.org). Three stop codons were identified in the natural DENV sequence which were recoded as follows: A10290→T, A10370→T, and T10423→A. Sequences corresponding to the constructs shown in **Figure 4** were purchased as gBlocks from IDT and cloned using Gibson cloning (NEB) into the BamHI site of the pYDL reporter. Specific sequences of any of the constructs is available by request from the authors.

Transformations into Yeast. Yeast cells intended for transformation, typically 50 ml, were grown to mid-log phase ($0.6 \geq OD_{600} \geq 1.0$) pelleted, resuspended and washed once with water**,** pelleted again and resuspended in 500 μl of 100 mM LiOAc. Cells were transferred to a 1.5 ml tube, again pelleted and finally resuspended in water for use in transformation reactions containing the following: 50 μl resuspended yeast, ~1 μg of plasmid DNA, 100 μg of sheared salmon sperm DNA, and 500 μl of PLATE buffer (40% PEG 3350, 100 mM LiOAc, 10 mM Tris pH 7.5, and 0.4 mM EDTA). Transformation reactions were incubated at 42 °C for 35 – 40 min then plated onto auxotrophic dropout agar. Plates were incubated at 30 °C for 2 days until a single colony could be picked and maintained for future experimentation and long-term storage.

RNA isolation: RNA was isolated from yeast by hot acid-phenol extraction. Briefly 10 ml of mid to late logarithmic phase ($0.6 \geq OD_{600} \geq 1.1$) culture in Y_{min} -ura was pelleted at 4°C at 3068 rcf. Cells were resuspended in 1 ml of cold Milli-Q grade, autoclaved, filtered water and transferred to screw top 1.5 ml tubes. Cells were pelleted by centrifugation at 6010 rcf in a tabletop microcentrifuge, decanted, and occasionally stored as pellets at -80°C prior to further processing. Pelleted cells were resuspended in 400 μl of TES (10 mM Tris, 1mM EDTA, 0.5% w/v sodium dodecyl sulfate) to which 400 μl of warm 5:1 Acid Phenol:Chloroform (Ambion, cat. # AM9722) were added and the resulting phase-separated mixture was agitated by vortexing at maximum speed for 15 sec. Samples were then incubated in a 65°C heat block for 30 min with periodic

vortexing prior to a 5 minute chill on ice and subsequent repartitioning at 18407 rcf at 4°C for 10 min. The aqueous supernatant was transferred to a new 2 ml screw-top tube to which 400 μl of 24:24:1 phenol:chloroform:isoamyl alcohol (Ambion cat. # 9732) was added. The resulting mixture was vortexed for 30 sec and again spun at 18407 rcf for 10 min. The resulting aqueous supernatant was again transferred to a new 2 ml tube and precipitated via the addition of 40 μl of 3 M sodium acetate pH 3.5 and 1000 μl 200 proof ethanol. Samples were incubated on dry ice or in an -80°C freezer for 2+ hours followed by centrifugation at 18407 rcf for at 30 min. The resulting supernatant was decanted and the RNA-containing pellet washed with 70% (v/v) aqueous ethanol prior to re-pelleting at 18407 rcf for 20 min at 4°C in a microcentrifuge. The resulting ethanolic supernatant was decanted and RNA pellets were dried by inversion of the open-capped tubes over a lint-free technical wipe for 30 min to an hour. Upon drying, RNA pellets were resuspended in 50 μl of autoclaved, DEPC-treated, filtered water typically yielding RNA concentrations of ≥2000 ng/μl. Isolated total RNA was diluted and aliquoted to 400 ng/μl, then frozen at -80°C.

Primer 5' end-labeling: To label DNA oligonucleotides used for primer extension experiments, oligonucleotides from IDT were received as lyophilized solids were resuspended and diluted to 5 μM. Labeling reactions were designed to use equimolar amounts of DNA and γ-^{32}P-ATP (Perkin Elmer cat. # NEG035C001MC) and consisted of 37.5 pmol (7.5 μl of 5 μM) DNA, 40 pmol ATP (1.5 μl of 27.66 μM), and 10 U of T4 PNK in the manufacturer's supplied conditions of 70 mM Tris-HCl,10 mM $MgCl_2$, 5 mM DTT at pH 7.6. Reactions were incubated for 1.5 hrs at 37°C. 150 μl of DEPC-treated water was then added and the reaction passed through a home-poured G-25 sephadex (GE Healthcare cat. # 17-0033-01) spin column. The DNA containing flow through of the procedure was then ethanol precipitated through the addition of 5 μl of high-concentration (>5mg/ml) carrier RNA, 30 μl of 3 M ammonium acetate and 560 μl of 200 proof alcohol. The mixture was incubated on dry ice for at least 2 hrs then pelleted by centrifugation at 21000 rcf at 2°C . The ethanolic supernatant was decanted, and the DNA-containing pelleted washed with 75% ethanol, centrifuged again, decanted, and then dried to completion via speed-vac. Prior to use ^{32}P-labeled primers were resuspended in 200 mM Tris pH 8, 200 mM NaCl, 40 mM DTT (6X anneal) buffer.

Primer extension: Primer extension of total yeast RNA was carried out by combining 12.5 μl of 400 ng/μl total yeast RNA with 2.5 μl of a mixture of ^{32}P labeled primers dissolved in 6X anneal buffer. Annealing of ^{32}P labeled primers took place in 33 mM Tris, pH 8.0, 33 mM NaCl, 6.67 mM DTT and was accomplished using a thermocycler program that heated to 90°C for 3 min, ramped to 55°C and held for 3 min, ramped to 4°C, and were then immediately plunged into liquid N_2. Prior to reverse transcription samples were thawed on ice then 15 μl of a reverse transcription solution (RT mix) containing 1.6 mM dNTPs, 167 mM Tris pH 8.3, 250 mM KCl,10 mM $MgCl_2$, 6 mM DTT, and 1 μl GoScript™ reverse transcriptase (Promega cat. # A5003) was added. The combined mixture was incubated at 42°C for 45 min, 55°C for 15 min, 65°C for 15 min in a thermocycler after which 3 μl of 100 mM NaOH was added and the reaction was incubated for an additional 3 min at 90°C. Lastly, 25 μl of 95% formamide, 5 mM EDTA loading dye was added and the reactions were incubated at 80°C for 3 min prior to being loaded onto a 6% (19:1 mono:bis acrylamide) sequencing gel and electrophoresed at 65 W for 2.5 hrs. The resulting gels were transferred to Whatman paper, dried and exposed to Molecular Dynamics phosphor screens before being imaged on a Storm 720 scanner. Gels were visualized using ImageQuant software.

***β*-galactosidase assays:** Liquid assays were performed as described before. Specifically, 1.5 ml of liquid cultures in SD (-Ura) media were harvested during late logarithmic growth (OD_{600} 0.8–1.2) and washed with Z buffer (60 mM Na_2HPO_4, 40 mM NaH_2PO_4,10 mM KCl, 1 mM $MgSO_4$ pH 7.0). Cells were resuspended in 100 μl of Z buffer and lysed by 6 cycles of freeze-thawing (alternating each 30 seconds between liquid N_2 and a 42°C water bath). Lysed cells were incubated with 700 μl of prewarmed (30°C) Z buffer that included 1 mg/ml ortho-nitrophenyl-β−galactopyranoside (ONPG) and 50 mM β-mercaptoethanol (BME). Reactions were incubated at 30°C for 3–4 hrs and stopped by the addition of 0.5 ml 1 M $NaCO_3$. Afterwards cell debris was pelleted and the OD_{420} of the supernatant was measured. Activity in Miller units was calculated as OD_{420} × 1,000 / OD_{600} × minutes elapsed × 1.5 ml. Activity in Miller units was corrected for background using lysates from cells lacking the IRES reporter.

Translation Assay: A single colony of yeast transformed with pYDL or pYDL-xrRNA modified reporters was used to inoculate an overnight culture in SD min (-Ura) plus 2% (w/v) glucose media. The following day that overnight culture was used to inoculate a fresh culture which was grown to an OD_{600} of 0.6 to 0.7 units at 30°C. A 1 ml sample of the culture was then removed, pelleted, washed once with phosphate buffered saline (137 mM NaCl, 2.7 mM KCl, 10 mM Na_2HPO_4, 1.8 KH_2PO_4 pH 7.4) plus protease inhibitors (Roche cat. #04693132001), pelleted again, and resuspended in PBS. Cells were lysed by repeated freeze-thaw cycles as described above for β-galactosidase assays. Cellular debris was then pelleted by centrifugation and either 5 μl or 10 μl of the clarified supernatant used in dual luciferase assays following the manufacturer's prescribed protocol (Promega, cat # E1910). Data are shown as the ratio of RLUC to FLUC activity averaged over six experiments.

REFERENCES:

1. Gygi SP, Rochon Y, Franza BR, Aebersold R. Correlation between protein and mRNA abundance in yeast. Mol. Cell. Biol. American Society for Microbiology (ASM); 1999 Mar;19(3):1720–30. PMCID: PMC83965

2. Liu Y, Beyer A, Aebersold R. On the Dependency of Cellular Protein Levels on mRNA Abundance. Cell. 2016 Apr 21;165(3):535–50.

3. Heck AM, Wilusz J. The Interplay between the RNA Decay and Translation Machinery in Eukaryotes. Cold Spring Harb Perspect Biol. Cold Spring Harbor Lab; 2018 May 1;10(5):a032839.

4. Gilbertson S, Federspiel JD, Hartenian E, Cristea IM, Glaunsinger B. Changes in mRNA abundance drive shuttling of RNA binding proteins, linking cytoplasmic RNA degradation to transcription. Elife. eLife Sciences Publications Limited; 2018 Oct 3;7:243. PMCID: PMC6203436

5. Haimovich G, Medina DA, Causse SZ, Garber M, Millán-Zambrano G, Barkai O, et al. Gene expression is circular: factors for mRNA degradation also foster mRNA synthesis. Cell. 2013 May 23;153(5):1000–11.

6. Sun M, Schwalb B, Pirkl N, Maier KC, Schenk A, Failmezger H, et al. Global analysis of eukaryotic mRNA degradation reveals Xrn1-dependent buffering of transcript levels. Mol. Cell. 2013 Oct 10;52(1):52–62.

7. Akiyama BM, Laurence HM, Massey AR, Costantino DA, Xie X, Yang Y, et al. Zika virus produces noncoding RNAs using a multi-pseudoknot structure that confounds a cellular exonuclease. Science. 2016 Dec 2;354(6316):1148–52. PMCID: PMC5476369

8. Chapman EG, Costantino DA, Rabe JL, Moon SL, Wilusz J, Nix JC, et al. The structural basis of pathogenic subgenomic flavivirus RNA (sfRNA) production. Science. American Association for the Advancement of Science; 2014 Apr 18;344(6181):307–10. PMCID: PMC4163914

9. Pijlman GP, Funk A, Kondratieva N, Leung J, Torres S, van der Aa L, et al. A highly structured, nuclease-resistant, noncoding RNA produced by flaviviruses is required for pathogenicity. Cell Host Microbe. 2008 Dec 11;4(6):579–91.

10. Slonchak A, Khromykh AA. Subgenomic flaviviral RNAs: What do we know after the first decade of research. Antiviral Res. 2018 Nov;159:13–25.

11. Chapman EG, Moon SL, Wilusz J, Kieft JS, Nilsen T. RNA structures that resist degradation by Xrn1 produce a pathogenic Dengue virus RNA. Elife. eLife Sciences Publications Limited; 2014 Apr 1;3:e01892. PMCID: PMC3968743

12. MacFadden A, O'Donoghue Z, Silva PAGC, Chapman EG, Olsthoorn RC, Sterken MG, et al. Mechanism and structural diversity of exoribonuclease-resistant RNA structures in flaviviral RNAs. Nature Communications. Nature Publishing Group; 2018 Jan 9;9(1):119. PMCID: PMC5760640

13. Steckelberg A-L, Vicens Q, Kieft JS. Exoribonuclease-Resistant RNAs Exist within both Coding and Noncoding Subgenomic RNAs. Idnurm A, editor. MBio. American Society for Microbiology; 2018 Dec 18;9(6):156. PMCID: PMC6299227

14. Charley PA, Wilusz CJ, Wilusz J. Identification of phlebovirus and arenavirus RNA sequences that stall and repress the exoribonuclease XRN1. J. Biol. Chem. 2018 Jan 5;293(1):285–95. PMCID: PMC5766927

15. Flobinus A, Chevigny N, Charley PA, Seissler T, Klein E, Bleykasten-Grosshans C, et al. Beet Necrotic Yellow Vein Virus Noncoding RNA Production Depends on a 5“→3” Xrn Exoribonuclease Activity. Viruses. Multidisciplinary Digital Publishing Institute; 2018 Mar 19;10(3):137. PMCID: PMC5869530

16. Moon SL, Blackinton JG, Anderson JR, Dozier MK, Dodd BJT, Keene JD, et al. XRN1 stalling in the 5' UTR of Hepatitis C virus and Bovine Viral Diarrhea virus is associated with dysregulated host mRNA stability. Siddiqui A, editor. PLoS Pathog. Public Library of Science; 2015 Mar;11(3):e1004708. PMCID: PMC4352041

17. Dilweg IW, Gultyaev AP, Olsthoorn RC. Structural features of an Xrn1-resistant plant virus RNA. RNA Biol. 2019 Apr 5;:1–8.

18. Boehm V, Gerbracht JV, Marx M-C, Gehring NH. Interrogating the degradation pathways of unstable mRNAs with XRN1-resistant sequences. Nature Communications. Nature Publishing Group; 2016 Dec 5;7(1):13691. PMCID: PMC5150221

19. Russo J, Mundell CT, Charley PA, Wilusz C, Wilusz J. Engineered viral RNA decay intermediates to assess XRN1-mediated decay. Methods. 2019 Feb 15;155:116–23. PMCID: PMC6387842

20. Spahn CMT, Jan E, Mulder A, Grassucci RA, Sarnow P, Frank J. Cryo-EM visualization of a viral internal ribosome entry site bound to human ribosomes: the IRES functions as an RNA-based translation factor. Cell. 2004 Aug 20;118(4):465–75.

21. Johnson AG, Grosely R, Petrov AN, Puglisi JD. Dynamics of IRES-mediated translation. Philos. Trans. R. Soc. Lond., B, Biol. Sci. 2017 Mar 19;372(1716):20160177. PMCID: PMC5311923

22. Thompson SR, Gulyas KD, Sarnow P. Internal initiation in Saccharomyces cerevisiae mediated by an initiator tRNA/eIF2-independent internal ribosome entry site element. PNAS. National Acad Sciences; 2001 Nov 6;98(23):12972–7.

23. Mayas RM, Maita H, Semlow DR, Staley JP. Spliceosome discards intermediates via the DEAH box ATPase Prp43p. Proc. Natl. Acad. Sci. U.S.A. 2010 Jun 1;107(22):10020–5. PMCID: PMC2890470

24. Hodgman CE, Jewett MC. Characterizing IGR IRES-mediated translation initiation for use in yeast cell-free protein synthesis. N Biotechnol. 2014 Sep 25;31(5):499–505.

25. Pestova TV, Hellen CUT. Reconstitution of eukaryotic translation elongation in vitro following initiation by internal ribosomal entry. Methods. 2005 Jul;36(3):261–9.

26. Kerr CH, Ma ZW, Jang CJ, Thompson SR, Jan E. Molecular analysis of the factorless internal ribosome entry site in Cricket Paralysis virus infection. Sci Rep. Nature Publishing Group; 2016 Nov 17;6(1):37319. PMCID: PMC5112510

27. Lesser CF, Guthrie C. Mutational analysis of pre-mRNA splicing in Saccharomyces cerevisiae using a sensitive new reporter gene, CUP1. Genetics. 1993 1993-04-01;133(4):851–63.

28. Harger JW, Dinman JD. An in vivo dual-luciferase assay system for studying translational recoding in the yeast Saccharomyces cerevisiae. RNA. Cold Spring Harbor Laboratory Press; 2003 Aug;9(8):1019–24. PMCID: PMC1236998

29. Furuichi Y, Shatkin AJ. Viral and cellular mRNA capping: past and prospects. Adv. Virus Res. 2000;55:135–84.

30. Shimotohno K, Kodama Y, Hashimoto J, Miura KI. Importance of 5'-terminal blocking structure to stabilize mRNA in eukaryotic protein synthesis. PNAS. National Academy of Sciences; 1977 Jul;74(7):2734–8. PMCID: PMC431268

31. Qu X, Wen J-D, Lancaster L, Noller HF, Bustamante C, Tinoco I. The ribosome uses two active mechanisms to unwind messenger RNA during translation. Nature. Nature Publishing Group; 2011 Jul 6;475(7354):118–21. PMCID: PMC4170678

32. Amiri H, Noller HF. Structural evidence for product stabilization by the ribosomal mRNA helicase. RNA. 2019 Mar;25(3):364–75. PMCID: PMC6380275

33. Xie P, Chen H. Mechanism of ribosome translation through mRNA secondary structures. Int. J. Biol. Sci. 2017;13(6):712–22. PMCID: PMC5485627

34. Betterton MD, Jülicher F. A motor that makes its own track: helicase unwinding of DNA. Phys. Rev. Lett. American Physical Society; 2003 Dec 19;91(25):258103.

35. Manosas M, Xi XG, Bensimon D, Croquette V. Active and passive mechanisms of helicases. Nucleic Acids Res. 2010 Sep;38(16):5518–26. PMCID: PMC2938219

36. Jinek M, Coyle SM, Doudna JA. Coupled 5' nucleotide recognition and processivity in Xrn1-mediated mRNA decay. Mol. Cell. Elsevier; 2011 Mar 4;41(5):600–8. PMCID: PMC3090138

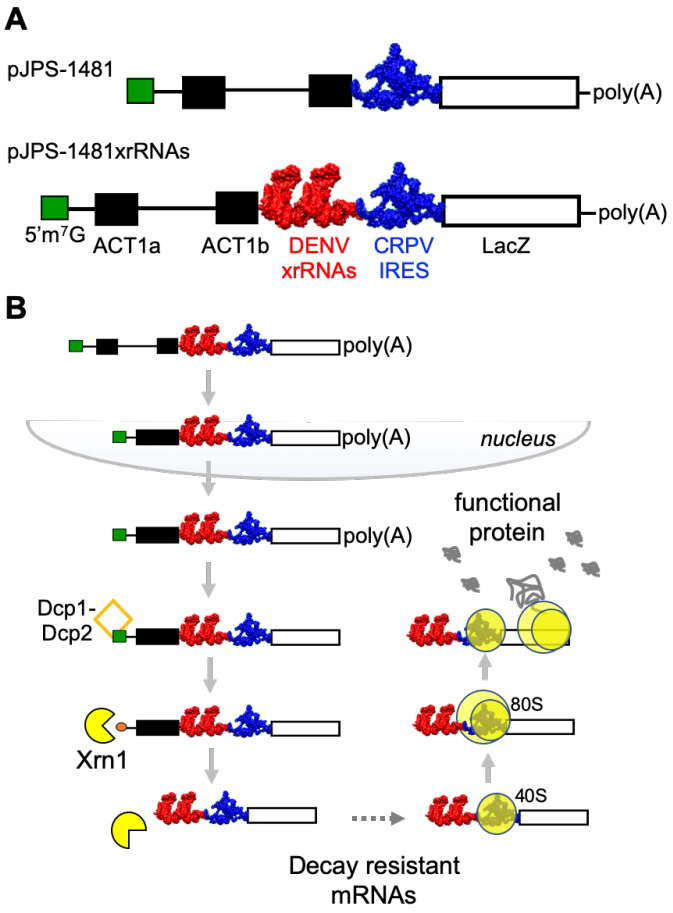

Figure 1: Outline for the expression of decay-resistant messenger RNAs. A) Layout of the pre-mRNA splicing reporters examined in this study. B) The metabolism of xrRNA-modified mRNAs: pre-mRNA transcripts are spliced within the nucleus and exported to the cytoplasm where they are eventually decapped and subject to decay by the 5'→3' exoribonuclease, Xrn1. Instead of being degraded however, the mRNAs created in this study harbor xrRNAs that prevent their decay and result in the build-up of products that include the CrPV IRES domain capable of driving cap-independent translation of a LacZ reporter.

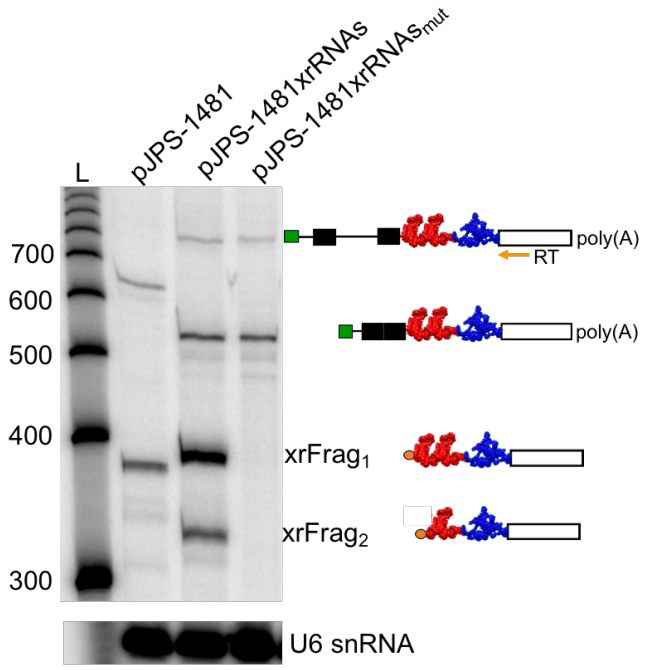

Figure 2: xrRNAs protect mRNAs from degradation. Primer extension analysis of *imt3 imt4* yeast expressing pJPS-1481 xrRNA-modified reporters. RT was carried out using total cellular RNA and a ^{32}P labeled primer complimentary to the 5' end of the LacZ gene. The resulting cDNA products were separated by denaturing PAGE. The RNA species portrayed to the right of the figure are those produced from pJPS-1481xrRNAs reporter. The darker and lighter bands observed in the pJPS-1481 lane represent the pJPS-1481 mRNA and pre-mRNA respectively. RT of U6 snRNA served as an internal control.

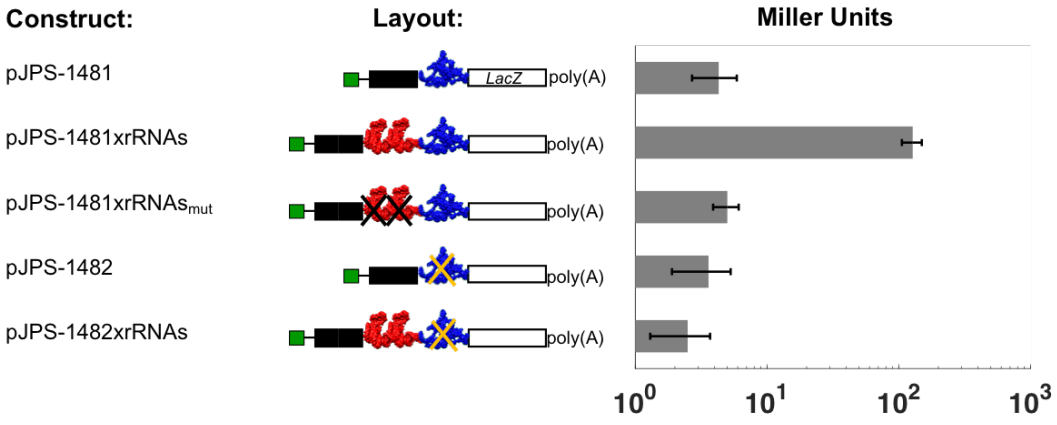

Figure 3: Partially-degraded RNAs undergo cap independent translation. *imt3 imt4* yeast expressing pJPS-1481, pJPS-1481xrRNAs and pJPS-1481xrRNAs$_{mut}$ as well as similar IRES-dead controls pJPS-1482 and pJPS-1482xrRNAs, were grown to mid-log phase, lysed and subjected to β-galactosidase assays as described in the Materials and Methods section. Lysates from cells expressing decay-resistant reporters show more than an order of magnitude increase in enzymatic activity.

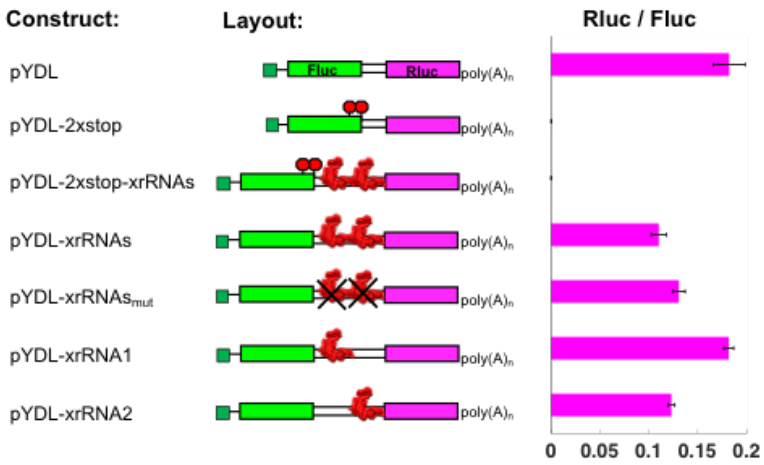

Figure 4: xrRNA structures do not block translation. The DENV xrRNA structures and related controls were inserted into pYDL dual-luciferase reporters shown above and expressed in CRY 1 yeast. Luciferase assays were performed using whole-cell lysates to yield the Rluc/Fluc ratios shown next to each construct. Rluc is shown by a magenta box, and Fluc is depicted by a green box. Starting from the top: first and second constructs lack xrRNAs, the third and fourth structures contain two copies of the DENV xrRNAs, the fifth structure contains two mutant copies of the xrRNAs, and the sixth and seventh constructs contain a single DENV xrRNA each. Stop codons are represented by small red octagons and mutation of the xrRNAs is indicated by strikethrough “X”.